25th ABCM International Congress of Mechanical Engineering
October 20-25, 2019, Uberlândia, MG, Brazil

COB-2019-1304
ANALYSIS OF THE WAKE OF TWO PARALLEL CIRCULAR CYLINDERS AT SEVERAL ANGULAR POSITIONS TO THE FLOW

Patrick Batista Habowski
Alexandre Vagtinski de Paula
Universidade Federal do Rio Grande do Sul, Programa de Pós-Graduação em Engenharia Mecânica (PROMEC), Rua Sarmento Leite, 425, Porto Alegre, CEP 90050-170, Brazil
patrick.habowski@ufrgs.br (P.B. Habowski), depaula@ufrgs.br (A.V. de Paula)

Sérgio Viçosa Möller
Universidade Federal do Rio Grande do Sul, Programa de Pós-Graduação em Engenharia Mecânica (PROMEC), Rua Sarmento Leite, 425, Porto Alegre, CEP 90050-170, Brazil
svmoller@ufrgs.br

Abstract. *An experimental study performed in an air channel using hot wire anemometers and a flow observation in a hydrodynamic channel is presented, for a configuration of two rigid cylinders with different angular positions to the flow. The main objective is to analyze the effects of flow incidence angles on the bistability, employing two different schemes of positioning of the hot wire anemometers. Bistability is a phenomenon which presents two distinct behaviors for the wake under the same conditions to the flow, occurring in some specific configurations, like two parallel cylinders placed side-by-side. In the first scheme analyzed, the anemometers had a fixed distance from the center of rotation axis and in the second one was used a movable table to modify the position every time the angle was changed. The discrete wavelets transform was applied in order to reconstruct the velocity signals. The results showed the presence of bistability only for side-by-side configuration, being clearer its observation with second measuring scheme. Through the flow visualization was possible to see the flow mode changes for side-by-side configuration, and for the other angles, the presence of a narrow and a wide wake were observed, but without flow mode changes, in accordance with the results in the air flow channel.*

Keywords: *Bistability Flow Phenomenon, Flow Visualization, Hot Wires, Turbulent Flow, Wavelets.*

1. INTRODUCTION

Circular cylinders are a common configuration that appears in many applications in industry and engineering, being a common geometry, for example, in pipelines, heat exchangers, transmission lines and nuclear reactors. When a configuration with two parallel circular cylinders of equal diameter, placed side-by-side, is submitted to a transversal flow, a random phenomenon is presented in the wake, since the relation between the diameter D and the pitch P, where P is the distance between the cylinder's centers, are around in the range 1.1 – 2.5, according to Alam et al. (2003) . This phenomenon is called bistability and presents a changing in the flow mode, as showed in Figure 1 (a), (b) and (c).

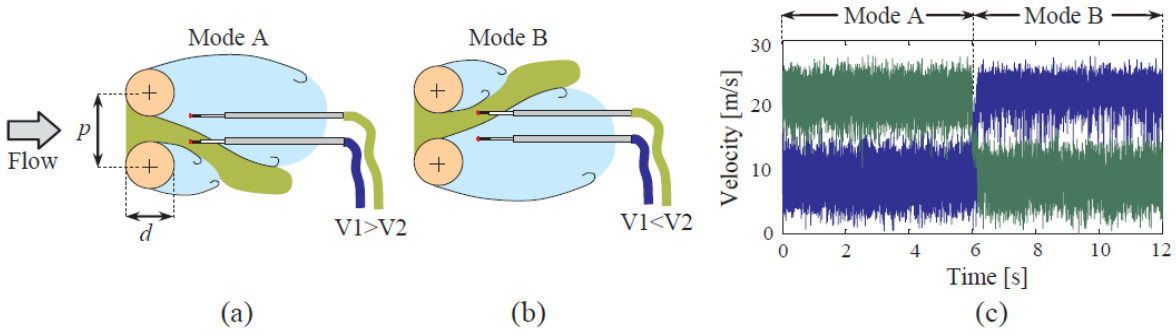

Figure 1 – Bistability modes (a) and (b), and the velocity vs. time chart of this phenomenon (c). Adapted from De Paula (2013).

In the Figure 1 (a) and (b) are shown the bistability phenomenon in the flow through the cylinders and in the Figure 1 (c) are shown the result of this characteristic in a velocity vs. time chart. Besides that, according to De Paula et al. (2013), this phenomenon generates two dominants vortex-shedding frequencies, each one associated with a wake, where the wide wake is associated with the lower frequency, and the narrow wake is associated with the higher frequency. Möller and de Paula (2018) presented a study showing that this phenomenon is chaotic for two circulars cylinders placed side-by-side and for two rows tube banks in triangular arrangement, i.e., it's independent of Reynolds number, cylinders misalignment or external influences.

Sumner (2010) presented a classification about the positioning of the cylinders in relationship to the flow. The classification is separated in tandem configuration, which cylinders are aligned horizontally, the side-by-side configuration, which the cylinders are aligned vertically, and, the last one, the staggered configuration, which the cylinders have an angle with the flow. Zdravkovich (1987) classified the flow according to the *T/D* and *L/D* ratio, where the author considered *T* and *L* as the vertical and horizontal distance from the center of the cylinders, respectively. This classification presents four regions: proximity interference, proximity and wake interference, wake interference and no interference. The study presented in this paper belongs to two regions along the experiment: the proximity interference, when it was in a side-by-side configuration, and in the proximity and wake interference, for the staggered one.

Alam and Sakamoto (2005) presented a study of staggered bodies, and results showed for the arrangement with about 5º with the flow that the gap flow is biased to one of the cylinders, and with 0º the gap flow is biased but switches intermittently to each cylinder. However, according to Alam and Zhou (2016), the bistability flow is highly sensitive to the flow incidence angle and the *P/D* ratio, occurring bistability phenomenon for 30° of flow incidence angle and *P/D* ratio equal 2.2, for example. The authors also related the bistable flow phenomenon to four switches physical phenomena: shear layer reattachment and rollup switch, the bubble formation and burst switch, shear layer switch and gap flow switch.

Varela et al. (2017) presented a study of bistability for a configuration of two rigid cylinders, placed in a rotational structure, performing discrete wavelets transform to the data acquired, and showed some results for this configuration using many different Reynolds numbers. For the results showed, there are more flow mode changings for the Reynolds number equal to 8.98×10^3, which is the lowest presented by the author. With the highest Reynolds numbers explored, the phenomenon occurs as well, but less often. Varela (2017) presented results for the visualization of the rotation for the configuration using a high-speed camera, where was showed the angle of the configuration in relationship with the time and was observed that the configuration of the two cylinders oscillates around the rotation axis for both directions until it rotates.

Results of flow visualization made by De Paula (2008) for two cylinders side-by-side and tube banks with 1.26 and 1.6 of *P/D* ratio showed the bistable phenomenon. The author performed the experiments for Reynolds number 7.5×10^3 and 1.5×10^4, blockage ratio equal to 25.3%, and the author perceived 2 – 4 flow mode changes in an observation time equal to 5 minutes. Destefani (2016) presented a study in a hydrodynamic channel with two parallel cylinders and diameter equal to 25.1 mm, in side-by-side position with 1.26 *P/D* ratio, and the results showed the bistability phenomenon occurs in horizontal and vertical positions as well. Also, the author made experiments during about 25 minutes in both cases, and the bistable phenomenon occurred just one or two times in this period, i.e., the number of occurrences is much less the in the air flow channel, in accordance with De Paula (2008).

Wong et al. (2014) investigated the dependence of the Reynolds number in a pattern of two rigid cylinders for several *P/D* ratios and angles between cylinder's centers and flow. The range of subcritical Reynolds was explored and results pointed out to appreciable effects involving the Reynolds number, considering flow separation, boundary layer thickness, gap flow deflection and vortex formation length. Neumeister et al. (2018a) examined the bistable phenomenon in two cylinders placed side-by-side with *P/D* ratio equal 1.26 and Reynolds number 2.2×10^4. The process of wake formation was described, where was found that the wake does not occurs simultaneously along the z-direction of the cylinder, i.e., there is a delay on the switching process. This characteristic is also presented in the cylinders wall pressure distribution, lift and drag coefficients.

This paper presents a study of bistable flow behavior for several flow incidence angles between the rotation perpendicular axis of the configuration with two rigid circular cylinders and the flow, as shown in Figure 3 (a), with the *P/D* ratio equal 1.26. In this study, was used an air flow channel with two hot wire probes, that were positioned in two different ways. It was also performed the discrete wavelet transform using the Matlab© software for post processing the data obtained. In order to better visualize the bistability phenomenon, visualization in a hydrodynamic channel was made, remaining the same characteristics for the channel and for the cylinders.

2. EXPERIMENTAL PROCEDURE

2.1 Air flow channel

The air flow channel employed in this study is made of acrylic glass, with a rectangular section of 0.193 m width, 0.146 m height and 2.29 m long, and is shown in Figure 2. The air flow is provided by a centrifugal blower of 0.64 kW and passes through a diffuser, two honeycombs and two screens, to reduce the flow turbulence intensity about 1%. The

two circular cylinders are made of PVC (PolyVinyl Chloride) with a diameter of 25.1 mm. The blockage ratio is 26% and the reference velocity is obtained with Pitot tube upstream the test section and generates a reference velocity of 10 m/s and a Reynolds number of 1.66×10^4.

The velocity of the flow was measured with a DANTEC StreamLine constant hot wire anemometry system and two hot wire probes, type DANTEC 55P11, which is designed with single wire perpendicular to the flow. The data acquisition was taken by a 16-bit A/D board, with USB interface, applying a sampling of 1000 Hz and a low pass filter at 300 Hz.

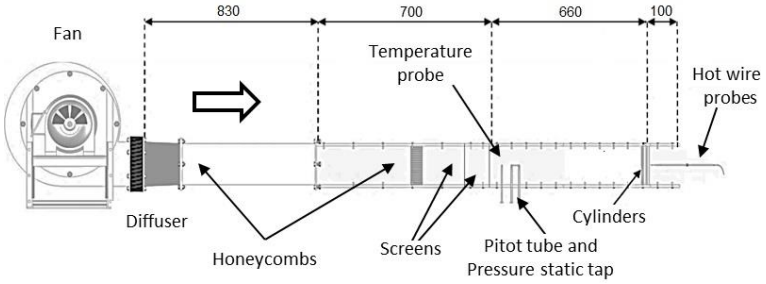

Figure 2 – Dimensions and details of the air channel.
Adapted from Neumeister el al. (2018b).

2.2 Analyzed angles

To determine the angles to perform this analysis was considered the "shadow angle", i.e., the angle between the line that crosses the two tangent walls of each cylinder with the center of the pitch *P* and the flow, as shown in Figure 3 (b). The "shadow angle" represents the angle which the distance between the two nearest walls of the cylinders is equal to zero considering a fixed point on the center of the air flow channel in a 2D view (Figure 3 c). For a two equal diameter cylinders of 25.1 mm and *P/D* ratio equal to 1.26, the "shadow angle" is equal to 36.75º. When the configuration is placed 36.75º with the flow, it means that the flow doesn't have a free space to flow parallel between the cylinders, just around them. Thus, it was defined the angles 0º (side-by-side configuration), 5º, 15º, 25º and 35º to perform the analysis.

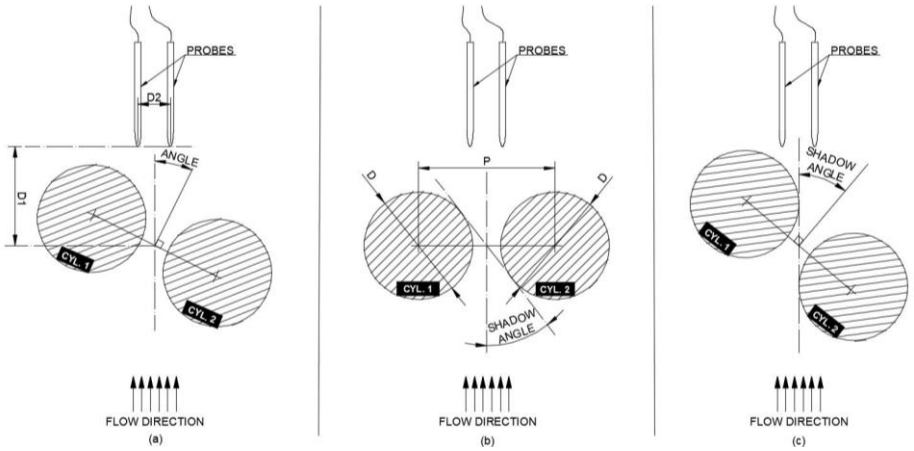

Figure 3 – Setup detail (a), scheme to define the "shadow angle" (b) and experiment built with "shadow angle" (c).

In order to acquire the signals of velocity, it's important to determine the position of the anemometers. So, it was defined two schemes for positioning the anemometers, using a movable table that allows the movement in x and y axes, with a scale which owns a resolution of 0.1 mm. In the first scheme, the anemometers were fixed in a defined distance from the rotation axis of the configuration equal to 30 mm (*D1* in Figure 3 a), which remains constant during the experiment. The second scheme, the distance was changed every time when the angle was modified. To determine this distance in every angle was considered an initial distance equal to 17 mm (*D1* in Figure 3 a) plus a displacement caused by the rotation of the configuration for every angle. The distance *D2* employed in Figure 3 (a) was 14 mm, and the midpoint of this distance was aligned with the rotation axis.

2.3 Flow visualization

Flow visualization was performed in a water channel with a closed circuit. The channel is made mainly of aluminum plate with 0.8 mm thickness, with a section made by acrylic glass where is taken the visualization trough a camera. The

dimensions are 3.25 m long with a rectangular section with 0.146 m height and 0.193 m width, the same section as the air flow channel. A set of two pumps of 0.37 kW each provides the water pumping, and can be used once at a time with a maximum flow rated of 160 L/min each. There is a mixer that collect the water pumped by each pump, a honeycomb for homogenize the flow, and an acrylic glass on top of the channel. The flow can be measured by means of a hydrometer, using together with a timer. Also, there are two ink tanks with colored water, which is injected in the flow downstream to the cylinders, through pipes with 3 mm of thickness which goes inside the cylinder, and the amount of colored water injected is controlled by two valves in each pipe line. This colored water is mixed with the clean water, then goes through the set of two cylinders and go back to a catch tank, where is pumped again to the flow. The Figure 4 presents a detailed view of the constructive form of the hydrodynamic flow channel.

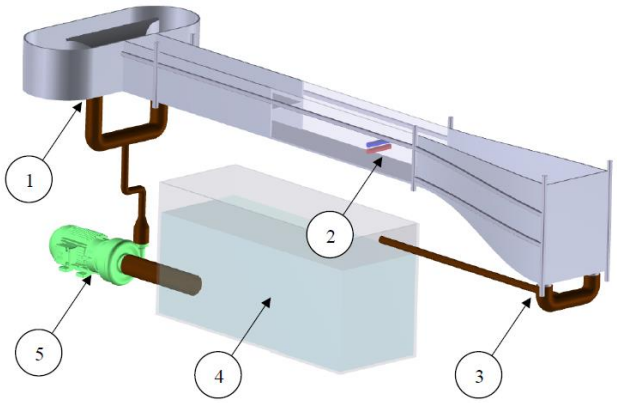

Figure 4 – Schematic of hydrodynamic flow channel for the visualization of the flow.
Adapted from Destefani (2016).

In the Figure 4, (1) represents the mixer of the water provided by each pump (5), (2) is where the visualization is taken with the colored water and (3) is the return water system to the catch tank (4). For the present work, it was employed flow visualization in vertical position and Reynolds number 5.05×10^3. The cylinders used in this experiment own the same characteristics of the ones used in the experiment in the air flow channel, but with two thin pipes inside them to release the colored water in the channel. The blockage ratio remains the same as the air flow channel, defined as 26%. For the video recorder, was used a camera with a resolution of 1080 x 720 pixels and 30 fps, and a tripod to fix the camera in an adequate height. Also, a mirror positioned 45° with the camera was fixed on the top of the channel to visualize the side view and the top view at the same time.

3. MATHEMATICAL REVIEW: WAVELETS

The wavelet analysis allows the study of a non-stationary signal in a time series domain and the detection of non-permanent flow structures. While the Fourier transform uses trigonometric functions as basis, like the sinus function, the basis of wavelets transforms, according Percival and Walden (2000), are functions called wavelets $\psi(t)$, with finite energy and zero average. The main idea of wavelet is the stretching and compressing the window of windowed Fourier transform, allowing the definition of the scales of interest in time and frequency domains (Neumeister et al., 2018b). The continuous wavelet transform (CWT) of a function $x(t)$ is given by Equation (1).

$$\tilde{X}(a,b) = \int_{-\infty}^{+\infty} x(t)\psi_{a,b}(t)\,dt \quad a,b \in \Re \tag{1}$$

In the Equation (1), $\tilde{X}(a,b)$ is the generic function in the wavelet domain, a and b are the wavelet parameters, $x(t)$ is a generic function in the time domain and the $\psi_{a,b}(t)$ is a generic wavelet function. The wavelet spectrum is defined by the matrix of squared wavelets coefficients, given by Equation (2). In the wavelet spectrum, the energy is related to each time and scale or frequency. So, this characteristic allows the representation of the energy of this transient signal over time and frequency domains, and is defined as spectrogram.

$$P_{xx}(a,b) = \left|\tilde{X}_{a,b}\right|^2 \tag{2}$$

In the Equation (2), $P_{xx}(a,b)$ is the wavelet spectrogram given by means of energy units. The discrete wavelet transform (DWT) is a sub sampling of continuous wavelets transform, but with dyadic scales, given by the Equation (3). According to Indrusiak (2004), the DWT decomposes the energy of the time series in the respective scales and the sum

showed in the Equation (3) could be seen as a portion of energy due the fluctuations in 2^{j-1} scale. Also, a time series and the discrete wavelet transform are both mathematical representations of an equal physical phenomenon.

$$\tilde{X}(j,k) = \sum_{t} x(t)\,\psi_{j,k}(t) \qquad j,k \in \Re \tag{3}$$

In the Equation (3), $\tilde{X}(j,k)$ is the wavelet series for the given *j* and *k* coefficients, *j* is the dilatation coefficient, *k* is the translation coefficient and the $\psi_{j,k}(t)$ is a generic wavelet function. According Indrusiak and Möller (2011), the length of the series restricts the number of coefficients, but the remaining ones are related to the lower frequencies, including the mean value of the signal, and cannot be disregarded. The DWT of a series with more than 2^j elements is calculated for $1 \leq j \leq J$, where *J* is a reasonable arbitrary choice, and is defined in Equation (4).

$$\tilde{X}(J,k) = \sum_{t} x(t)\,\phi_{J,k}(t) \tag{4}$$

In the Equation (4), $\phi_{J,k}(t)$ is the scaling function associated to the wavelet function. Therefore, any discrete time series with a sampling frequency (*Fs*) can be represented by Equation (5).

$$x(t) = \sum_{k} \tilde{X}(J,k)\phi_{J,k}(t) + \sum_{J\leq 1}\sum_{k} \tilde{X}(j,k)\phi_{J,k}(t) \tag{5}$$

In the Equation (5), the first term is the approximation of the signal at the scale J, corresponding to the frequency interval [0, $Fs/2^{J+1}$], and the second term is the details of the signal at the scales *j*, corresponding to the frequency intervals [$Fs/2^{j+1}$, $Fs/2^{j}$]. In the present work, were used Db20 wavelet and a level 8 (*J=8*) to reconstruct the signals.

4. RESULTS AND DISCUSSION

4.1 Velocity signals

The velocity signals were acquired in the air flow channel with two hot wire probes for several flow incidence angles. The results of signals employing the two schemes of positioning the probes for the side-by-side configuration are shown in Figure 5, for movable and fixed probe schemes (a and b, respectively). There is a large and visible difference between the signals, once the distance *D1* mentioned before is different for these schemes, being lesser for the movable probe scheme.

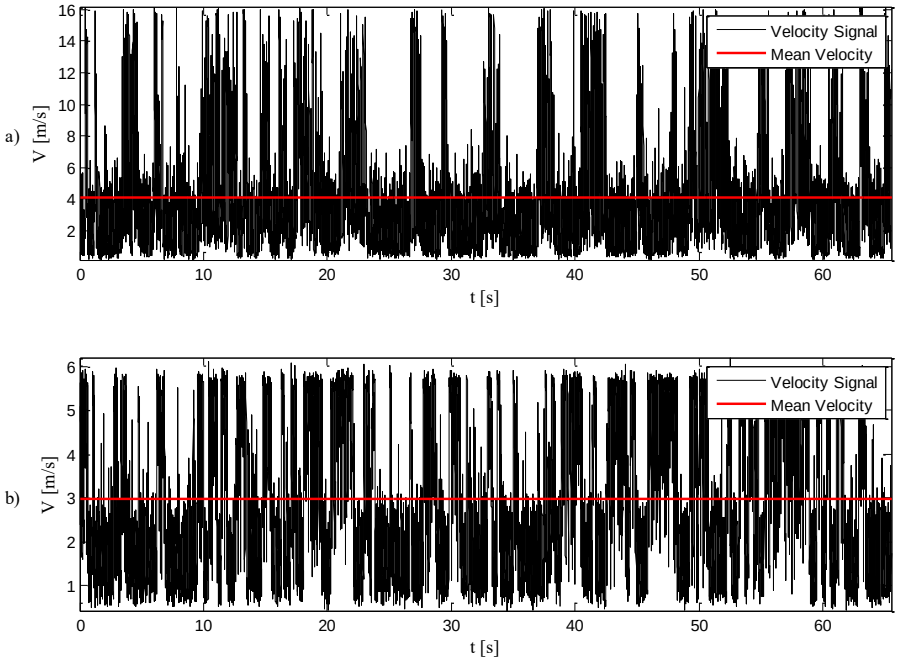

Figure 5 – Velocity signals acquired in the air flow channel with hot wire anemometers for movable probe scheme (a) and fixed probe scheme (b).

The maximum and the mean velocity for the movable probe scheme (Figure 5 a) are 16.19 m/s and 4.1 m/s, respectively, and for the fixed probe scheme (Figure 5 b), the maximum and the mean velocity are 6.21 m/s and 2.99 m/s, respectively. As expected, how much closer the cylinders, bigger is the velocity, so, the peaks and the mean velocity is bigger for the movable probe scheme (Figure 5 a). Despite this difference in the velocity quantities, the bistable phenomenon is clearly perceived in both cases, and in both data was applied the discrete wavelets transforms to a better understanding of the velocity values and the formation of different flow modes.

4.2 Reconstructed signals

In both probe positioning schemes, was used the discrete wavelet transform (DWT) to perform the reconstruction of the velocity signals. Also, it was employed Db20 wavelet type and level 8 for all the angles. The results for the fixed probe scheme are shown in Figure 6 and is possible to see the presence of bistability phenomenon for the angle 0º and some attempts of flow mode changes for the angle 5º. For 0º is counted about 45 flow mode changes and for the angle 5º is counted 4 attempts of flow mode changes. In the other angles, the presence of bistability was not perceived, but for the angles 25º and 35º there are two different levels of velocities, suggesting that the probes were in different flow modes.

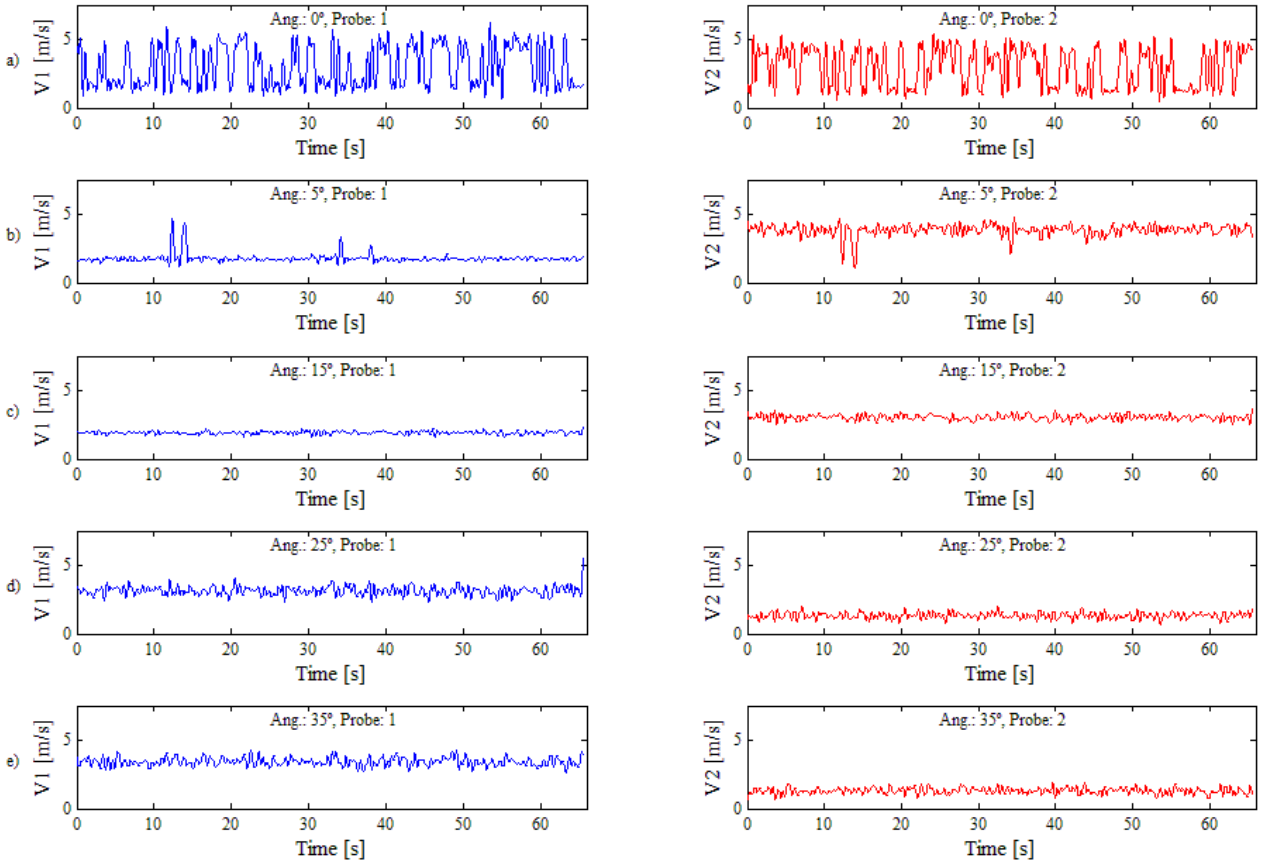

Figure 6 – Reconstructed signals for fixed probes employing discrete wavelet transform since 0º (a) to 35º (e).

For movable probes, was employed the same analysis as used for the fixed probes and the results are shown in Figure 7. It's possible to see the presence of bistability phenomenon for the angle 0º and some attempts of flow mode change for the angle 5º, as well as observed on the fixed probes scheme, and no one flow mode changes for the other angles. For the angle 0º is counted about 33 flow mode changes, and for the angle 5º is counted 6 attempts of flow mode changes. There is the presence of two different flow modes when the bistability phenomenon isn't perceived, but in this case, it occurs for the angle 15º.

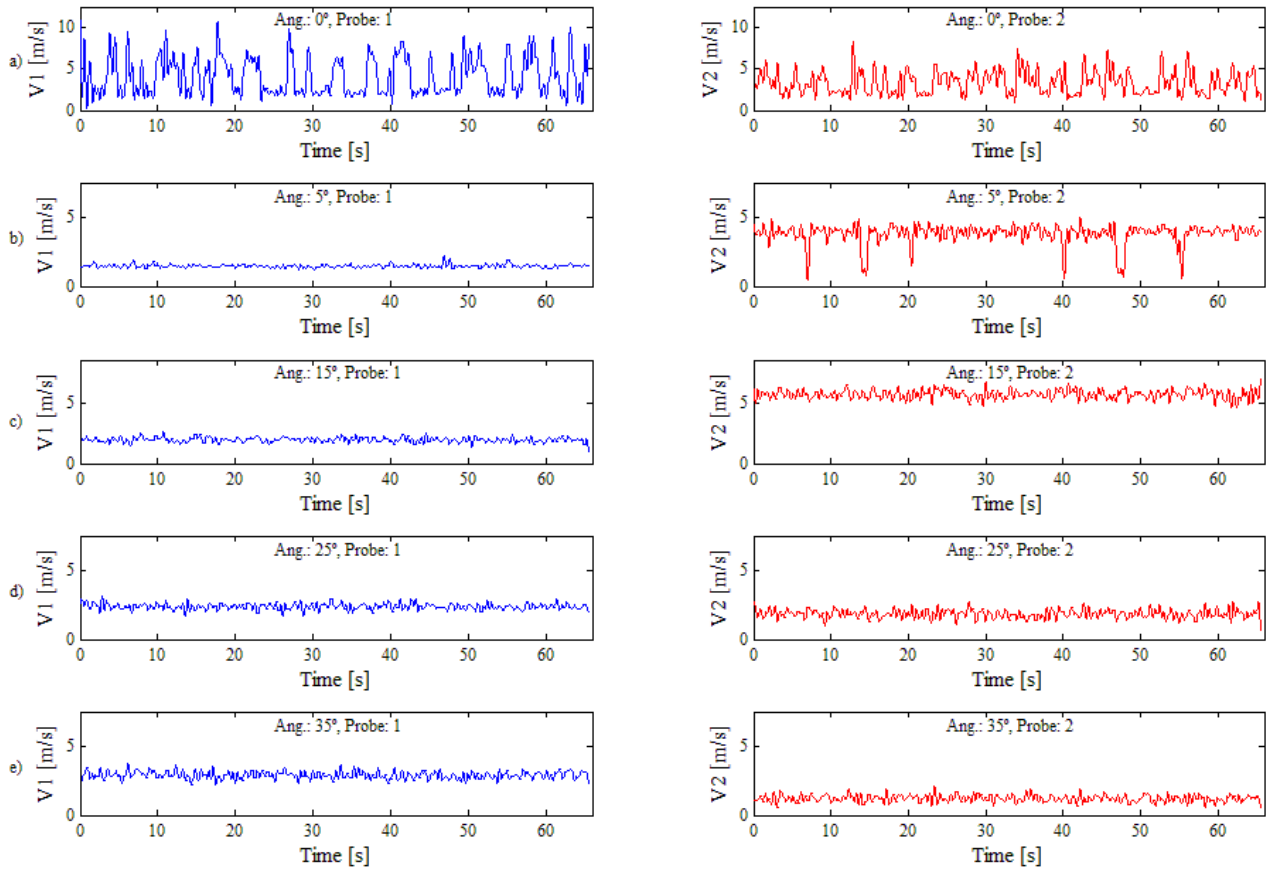

Figure 7 – Reconstructed signals for movable probes employing discrete wavelet transform since 0º (a) to 35º (e).

The spectrogram generated by continuous wavelets transform is shown in Figure 8, for the velocity signal of Figure 5 (a), which represents the velocity signal of probe 1 for the side-by-side configuration with distance *D1* equal to 17 mm. This spectrogram shows the energy distribution in a frequency interval from 1 to 250 Hz, with a bandwidth of 1 Hz and the time, with reconstructed velocity plotted over the chart. The highest values of energy in the arbitrary scale are reddish, as showed in the color bar, and are related to the highest values of velocity (kinetic energy). The lowest values of energy in the arbitrary scale are bluish, and are related to the lowest values of velocity.

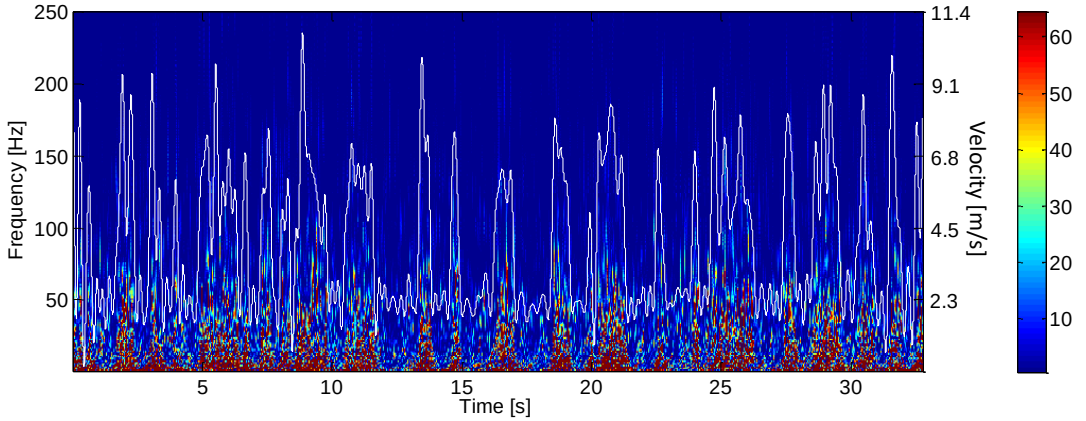

Figure 8 – Spectrogram for the velocity signal for side-by-side configuration.

Since one of the probes switches between the gap flow and the wide wake (Figure 1), and the gap flow corresponds to the peaks of velocity, the Figure 8 shows when the direction of gap flow changes to the wide wake (lowest velocities), there is a decreasing in the energy followed by a concentration of energy in frequencies below 20 Hz. In addition, in the gap flow (highest velocities), the energy is concentrated in a band of 25 – 80 Hz. These results show that the wide wake has a bigger concentration of energy in the lower values of energy, and are in according with

De Paula and Möller (2013). Also, the Strouhal numbers (S_t) were computed for the gap velocity (13.60 m/s) and the tube diameter, showing the S_t = 0.1 for the first frequency peak of energy observed from the Fourier frequency spectrum (f_s = 54.7 Hz), corresponding to the wide wake, and S_t = 0.33 for the narrow wake (f_s = 179.7 Hz). Another peak was found at f_s = 106.4 Hz, corresponding to the S_t = 0.195, and according to Alam et al. (2003), this Strouhal number correspond to an intermediate state of energy found by the authors in bistable phenomenon.

4.3 Flow visualization

Visualization in a hydrodynamic flow channel was performed with Reynolds number equal to 5.05x10³ and the same geometry for the cylinders and for the channel as employed in the air flow channel. Despite the fact of the Reynolds numbers are different between the experiments performed in hydrodynamic and air channel, both are included in the subcritical flow range (Blevins, 1990), resulting in wakes with similar characteristics. Through the flow visualization, was possible to see the two wakes developed by this phenomenon, and for the angle 0° was visible the changes in flow modes, in accordance with the results presented for the air flow channel in the Figure 6 and Figure 7. A time-lapse about the bistability phenomenon for the side-by-side position is shown in Figure 9.

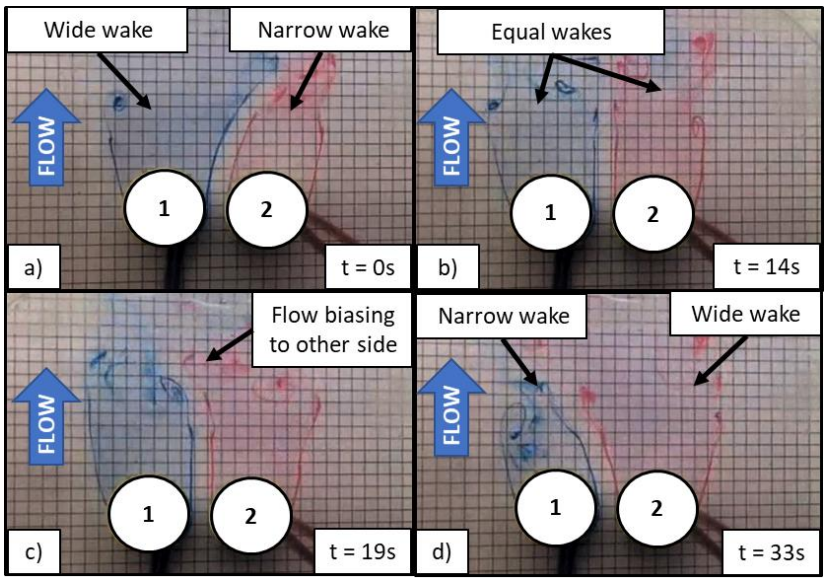

Figure 9 – Time-lapse for the visualization of the bistable flow phenomenon (side-by-side position).

During the process shown in Figure 9, the wake in the cylinder 1 is 40 mm width and the wake in the cylinder 2 is 30 mm width in the beginning of the observation time considered in Figure 9 (a). Then, the flow became instable, with the wakes oscillating between the states of Figure 9 (a) and (b), until the flow had been a low bit biased to the left side (Figure 9 c) and, finally, became stable in another flow mode (Figure 9 d), where the wake in the cylinder 1 is 30 mm width and the wake in the cylinder 2 is 42 mm width. This phenomenon occurred just one time during whole observation time, about 25 minutes. It was also observed the oscillation between the states of Figure 9 (a) and (b) more times, but without flow mode changes in these occurrences. These results are in agreement with those found by of De Paula (2008) and Destefani (2013).

In the other angles, the gap flow was biased according to the flow incidence angle, and wasn't perceive any flow mode changes, in accordance with the results presented for the air flow channel in the Figure 6 and Figure 7. The gap flow remains biased for the flow incidence angles equal to 5°, 15°, 25° and 35° during all the experiment. In the Figure 10 is showed the top and side views for the angle 15°, and is possible to see the two different wakes in the Figure 10 (a): a narrow wake, with about 30 mm of width, and a wide wake, with 43 mm of width. In the Figure 10 (b), the flow in blue color is biased to downside, and this oscillated upwards and downwards during the observation time.

The flow incidence angle 5° was a topic of interest with the results in the Figure 6 and Figure 7 and the results of flow visualization. In these figures, the results of velocity shown some attempts to changing the flow mode, but the flow is stable just in one mode. The results of flow visualization for 5° showed just one stable mode, with the gap flow biased during all the experiment, being very similar to behavior of angle 15°, shown in the Figure 10, and several disturbances in the wake were observed, even in the vertical direction (Figure 10 b). The results for this flow incidence angle can be compared with the results obtained by De Paula and Möller (2013), where the flow have two stable states, but the authors found a path that the flow tries to switch from an initial stable mode to another one, but cannot achieve this second state, and then goes back to the first. It suggests the presence of more than two flow modes, as observed previously by Alam et al. (2003).

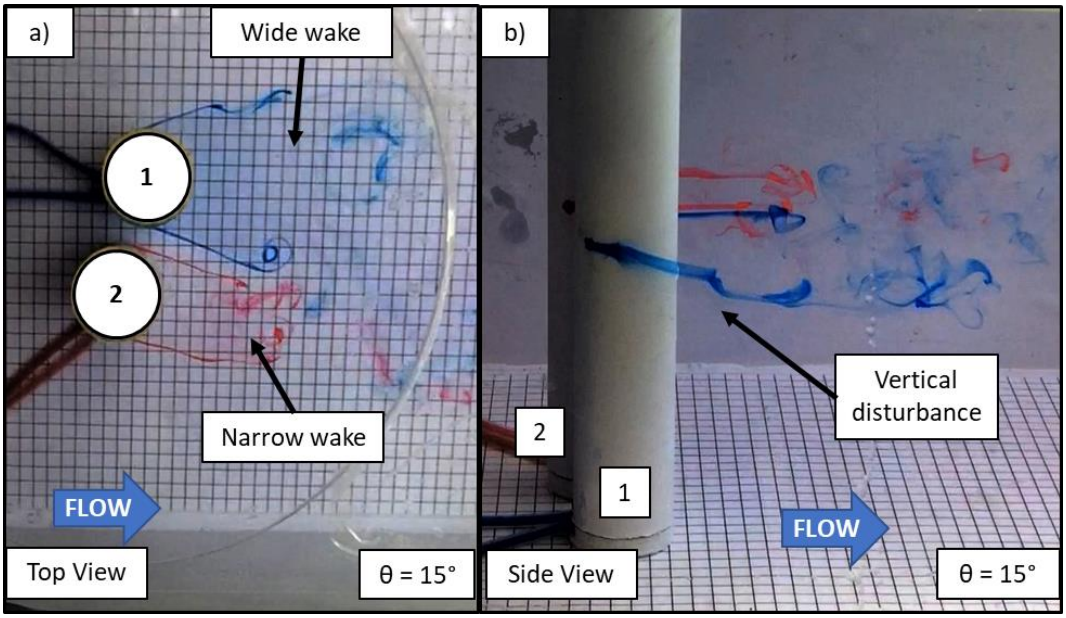

Figure 10 – Configuration with two different wakes: a narrow and a wide one (a), and the side view of the cylinders (b) for the flow incidence angle equal to 15°.

5. CONCLUSIONS

This work presents an experimental study about the bistable phenomenon through two circular cylinders placed at several flow incidence angles. The 1.26 *P/D* ratio remained constant during the experiments, and several flow incidence angles were applied to analyze the presence or no of the bistability phenomenon. The experiments were made in an air flow channel employing hot wire anemometers technique, and in a hydrodynamic flow channel, employing colored water to visualization of the wakes and bistable phenomenon. The blockage ratio was remained constant as 26% in both experiments, as well the geometry of the cylinders and for the channel. Besides the high blockage ratio, the switching phenomenon was not influenced by this factor.

In the air flow channel was considered two schemes to positioning the probes, with different distances from the rotation axis of the configuration. With the velocity signals obtained in the air flow channel, was possible analyze the differences in the peak and in the mean value of velocity for these positioning schemes, where was found bigger values for both quantities in the movable configuration, which is the closest of the rotation axis of the configuration for all the angles. Also, with the results obtained was performed wavelet transforms for every flow incidence angle and for both positioning schemes, in order to analyze the bistable phenomenon. It was found the bistable phenomenon just for the side-by-side configuration, and in the other angles was perceived the formation of two wakes, but without switching phenomenon. For the flow incidence 5° was perceived some attempts of flow mode change, but a second and stable mode was not achieved in this experiment.

For the side-by-side configuration was performed constant wavelet transform (CWT) in order to analyze the relationship between the scales of energy, frequency and time. This analysis pointed to an energy concentration for frequencies below 20 Hz for the wide wake (lowest velocities) and an energy concentration between 25 – 80 Hz for the gap flow (biggest velocities). It was also determined the Strouhal number, and was computed S_t = 0.1 and S_t = 0.33 for wide and narrow wakes, respectively, and S_t = 0.19, that is an intermediate state of energy between the switching phenomenon.

Through the hydrodynamic flow channel was possible to visualize the wide and narrow wakes and the bistability phenomenon. For this experiment, was observed the bistable phenomenon for side-by-side configuration and for the others was observed just the formation of the wide and the narrow wakes. These results are in agreement with the results obtained by the hot wire anemometer technique, and showed that the bistable phenomenon, for this case, is restricted to side-by-side configuration.

With the results analyzed, future work contemplating a better resolution between the side-by-side position and the angle 5º will be carried out to analyze until the bistable phenomenon remains. Also, more angles between the side-by-side position and tandem position will be performed, and more conclusions about the flow visualization will be made.

6. ACKNOWLEDGEMENTS

This study was financed in part by the Coordenação de Aperfeiçoamento de Pessoal de Nível Superior - Brasil (CAPES) - Finance Code 001.

7. REFERENCES

Alam, M.M., Moriya, M. and Sakamoto, H., 2003. "Aerodynamic chatacteristics of two side-by-side circular cylinders and application of wavelet analysis on the switching phenomenon". *Journal of Fluids and Structures 18,* pp. 325-346.

Alam, M.M. and Sakamoto, H., 2005. "Investigation of Strouhal frequencies of two staggered bluff bodies and detection of multistable flow by wavelets". *Journal of Fluids and Structures 20*, pp. 425-449.

Alam, M.M. and Zhou, Y., 2016. "Wake of two interacting circular cylinders: A review". *International Journal of Heat and Fluid Flow 62*, pp. 510-537.

Blevins, R.D., 1990. *Flow-induced vibration*. Van Nostrand Reinhold, New York, 2nd edition.

De Paula, A.V., 2008. Estudo sobre o fenômeno da biestabilidade de escoamentos turbulentos em bancos de tubos de arranjo triangular. Master's Degree thesis, Universidade Federal do Rio Grande do Sul, Porto Alegre, Brasil. Available in https://lume.ufrgs.br/handle/10183/16309.

De Paula, A.V., 2013. *Determinação de parâmetros que caracterizam o fenômeno da biestabilidade em escoamentos turbulentos*. Doctor's Degree thesis, Universidade Federal do Rio Grande do Sul, Porto Alegre, Brasil. Available in https://lume.ufrgs.br/handle/10183/72928.

De Paula, A.V. and Möller, S.V., 2013. "Finite mixture applied in the analysis of a turbulent bistable flow on two parallel circular cylinders". *Nuclear Engineering and Design*, Vol. 264, pp. 203-213.

De Paula, A.V., Endres, L.A.M. and Möller, S.V., 2013. "Experimental study of the bistability in the wake behind three cylinders in triangular arrangement". Technical paper of *The Brazilian Society of Mechanical Sciences and Engineering*.

De Paula, A.V. and Möller, S.V., 2018. "On the chaotic nature of bistable flows". *Experimental Thermal and Fluid Science*, Vol. 94, pp. 172-191.

Destefani, B.V., 2016. *Visualização da biestabilidade em dois cilindros circulares dispostos lado a lado em um canal hidráulico posicionados na horizontal e na vertical*. Monography for mechanical engineer's degree, Universidade Federal do Rio Grande do Sul, Porto Alegre, Brasil. Available in https://lume.ufrgs.br/handle/10183/148746.

Indrusiak, M.L.S., 2004. "*Caracterização de escoamentos turbulentos transientes usando a transformada de ondaletas*". Doctor's Degree thesis, Universidade Federal do Rio Grande do Sul, Porto Alegre, Brasil. Available in https://lume.ufrgs.br/handle/10183/4667.

Indrusiak, M.L.S. and Möller, S.V., 2011. "Wavelet analysis of unsteady flows: Application on the determination of the Strouhal number of the transient wake behind a single cylinder". *Experimental Thermal and Fluid Science 35,* pp. 319-327.

Neumeister, R.F., Ost, A.P. and Möller, S.V., 2018a. "Characteristics of the wake after a cylinder trip wire on turbulent crossflow". *11th Spring School on Transition and Turbulence – EPTT 2018.* Uberlândia, Brazil.

Neumeister, R.F., Petry, A.P. and Möller, S.V., 2018b. "Characteristics of the wake formation and force distribution of the bistable flow on two cylinders side-by-side". *Journal of the Brazilian Society of Mechanical Sciences and Engineering 40:564.*

Percival, D.B. and Walden, A.T, 2000. *Wavelet method for time series analysis*. Cambridge University Press, New York, 1st edition.

Sumner, D., 2010. "Two circular cylinders in cross flow: a review". *Journal of Fluids and Structures 26,* pp. 849-899.

Varela, D.J.C., 2017. *Análise experimental do escoamento transversal turbulento sobre dois cilindros paralelos fixos, com liberdade oscilatória e rotacional*. Master's Degree thesis, Universidade Federal do Rio Grande do Sul, Porto Alegre, Brasil. Available in https://lume.ufrgs.br/handle/10183/178285.

Varela, D.J.C, Neumeister, R.F., Dias, G.C., De Paula, A.V. and Möller, S.V., 2017. "Experimental analysis of turbulent transversal flow on two fixed parallel cylinders with oscillatory and rotational freedom". *COBEM 2017 - 24th ABCM International Congress of Mechanical Engineering*, Curitiba - Brazil.

Wong, C.W., Zhou, Y., Alam, M.M. and Zhou, T.M., 2014. "Dependence of flow classification on the Reynolds number for a two-cylinder wake". *Journal of Fluids and Structures 49,* pp.485-497.

Zdravkovich, M.M., 1987. "The effects of interference between circular cylinders in cross flow". *Journal of Fluids and Structures 1,* pp. 239-261.

8. RESPONSIBILITY NOTICE

The authors are the only responsible for the printed material included in this paper.